Relative Merits of Two Methods of Sample Introduction in Inductively Coupled Plasma Mass Spectrometry: Electrothermal Vaporisation and Direct Sample Insertion*

Gwendy E. M. Hall and Jean-Claude Pelchat
Geological Survey of Canada, 601 Booth Street, Ottawa, Ontario K1A 0E8, Canada

Dave W. Boomer and Mark Powell
Ontario Ministry of the Environment, Trace Contaminants Section, Toronto, Ontario M9W 5L1, Canada

Two alternative sample-introduction techniques to conventional nebulisation in analysis by inductively coupled plasma mass spectrometry, namely, electrothermal vaporisation and wire loop direct sample insertion, are compared. Both enjoy certain advantages over pneumatic nebulisation; these include a low sample volume requirement, higher sensitivity and reduced oxide and hydroxide formation. Although introduction by direct sample insertion is not subject to loss of analyte during transport to the plasma, it is less applicable to the analysis of solutions with significant concentrations of salt (higher than 1%) than electrothermal vaporisation is. Performances are compared in the analysis of the river water reference material SLRS-1, directly for Mn, As and Pd and for Au after extraction of the chloride complex $AuCl_4^-$ into isobutyl methyl ketone. Impurities of Fe, Mo and Ni in the wire loop precluded their determination by direct sample insertion.

Keywords: *Inductively coupled plasma mass spectrometry; electrothermal vaporisation; direction sample insertion*

Inductively coupled plasma mass spectrometry (ICP-MS) has provided the analytical chemist with the power to detect and quantify a wide range of elements at extremely low concentrations. Although this technique has improved potential for analysis, there remain some areas of analysis which are not served adequately. Notably, those areas requiring the use of a small sample size and those necessitating even lower detection limits would benefit from the development of a sample-introduction system designed with these requirements in mind. Conventional pneumatic nebulisation suffers from a number of shortcomings, *e.g.*, a low sample-transport efficiency of several per cent. Interferences in ICP-MS can be categorised into two broad classes: spectral overlap and non-spectral matrix-induced intensity changes. The former, arising from the formation of polyatomic and monatomic species that originate from the sample matrix and/or plasma gas, is now well documented.[1–3] The latter is more difficult to predict, although definite trends have been described in various studies.[4–6] Although both types of interference can often be minimised to a certain extent by control of the operating conditions in nebulisation (NEB) ICP-MS,[7–9] alternative methods of sample introduction could also reduce the severity of such problems. Several workers are investigating different sample introduction techniques,[10–17] including electrothermal vaporisation (ETV)[13–16] and direct sample insertion (DSI),[17] both of which have been studied previously in conjunction with analysis by ICP atomic emission spectrometry (ICP-AES).[18]

Research on DSI is being carried out at the Ontario Ministry of the Environment (MOE) and the Geological Survey of Canada (GSC) is studying ETV. The DSI device under investigation here is the wire loop originally designed by Salin and Sing[19]; the graphite electrode or cup described in ICP-AES studies has not yet been applied to ICP-MS. This paper summarises some recent collaborative work, carried out in both laboratories, in which the objective was to compare the two techniques with respect to precision, sensitivity, signal duration, versatility and susceptibility to interference effects.

* Presented at the 1988 Winter Conference on Plasma Spectrochemistry, San Diego, CA, USA, 3rd–9th January, 1988. GSC contribution 50487.

Experimental

Instrumentation

The ICP mass spectrometer used for this work was an ELAN 250 (Perkin-Elmer/SCIEX Instruments, Thornhill, Ontario, Canada) and has been described previously.[13]

ETV device

A schematic diagram of the ETV device is shown in Fig. 1. Either a custom-made graphite platform (flat or V-shaped) or a 20-mm long metal filament (tantalum, tungsten or rhenium) is heated resistively with a modified IL555 power supply (Instrumentation Laboratory, Lexington, MA, USA). The electrodes are cooled by water passing through the copper

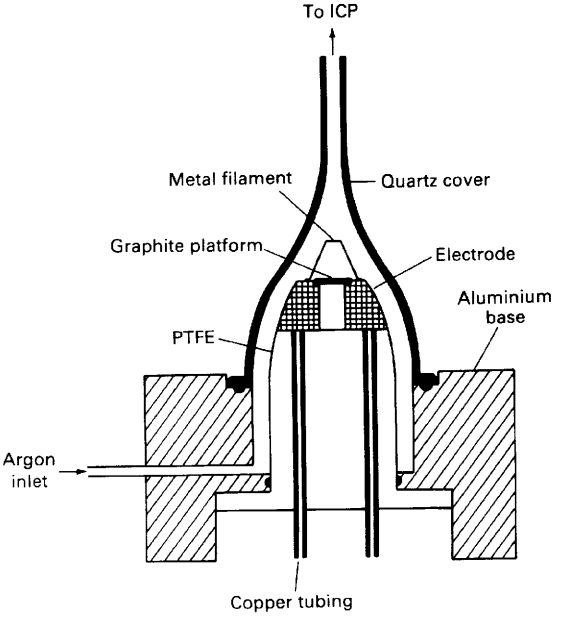

Fig. 1. Schematic diagram of the electrothermal vaporisation device

tubing (Fig. 1). The argon carrier gas is introduced tangentially at the base of the cell, producing a swirling motion which entrains the volatilised sample in a constrained flow pattern above the filament and sweeps it into the Tygon tubing (5 mm i.d., 50 cm length) leading to the plasma. The optimum volume (5–10 ml) in the glass dome above the filament has been designed to minimise dilution of the sample gas with the argon carrier gas at the same time allowing for condensation of vapours to a particulate size of about 1 μm before they reach the dome or tubing surfaces. Vapours generated during drying, ashing and cleaning steps are vented to waste while an auxiliary flow of argon (about 1.5 l min^{-1}) bypasses the ETV chamber and enters the plasma. The vapours generated during vaporisation of the analyte are swept into the ICP via a three-way stopcock that is automatically activated at the initiation of this step. Another ETV device has been designed which, unlike that shown in Fig. 1, has a second set of copper tubes through which a gas such as trifluoromethane (Freon) or hydrogen flows, entering the cell on both sides of the platform or filament. This optional flow is also activated automatically at the beginning of the vaporisation step.

Wire loop DSI device

A schematic diagram of the DSI device is shown in Fig. 2. The loop is fashioned from tungsten wire into a double circle and embedded, by heating, on a glass rod; this is then positioned firmly in its support with a pin vice. The sample is pipetted on to the loop which is transferred horizontally, via a computer-controlled stepping motor, through the solenoid-driven flow (auxiliary) stopper into the central tube of the torch. At the first stop, some distance below the plasma, drying takes place and then the loop is inserted quickly into the core of the plasma for vaporisation. The sequencing of stop positions and times for drying, ashing (if required) and vaporisation is accomplished by a microprocessor; reproducibility of positioning is excellent. Following vaporisation, the loop is retracted to the point of entry of the auxiliary argon for 10 s before returning to the sampling position. This cooling period in an argon atmosphere prolongs the lifetime of the loop to an average of about 100 firings.

Optimisation

ETV device

The critical parameters affecting sensitivity in sample introduction by ETV consist of the argon carrier gas flow-rate, the temperature of vaporisation, the r.f. power to the plasma and the injection rate when an auxiliary gas, such as Freon, is added. Changes in ion count rates with variations in the settings of these parameters have been demonstrated in previous publications.[14,20] The ion lens voltage settings are optimised during nebulisation of a standard solution of the particular analyte under investigation and it is found, generally, that further refinement for ETV introduction is not extensive. The choice of filament depends on the following: the volatility of the analyte, graphite being necessary for the high boiling-point elements; the nature of the solution (acidic, basic, organic); the possible formation of a filament-material species which is isobaric with the analyte (*e.g.*, $^{187}Re^{16}O^+$ on $^{203}Tl^+$ and $^{181}Ta^{16}O^+$ on $^{197}Au^+$); interaction between the analyte and the filament (*e.g.*, alloying); and analyte impurity in the filament material.

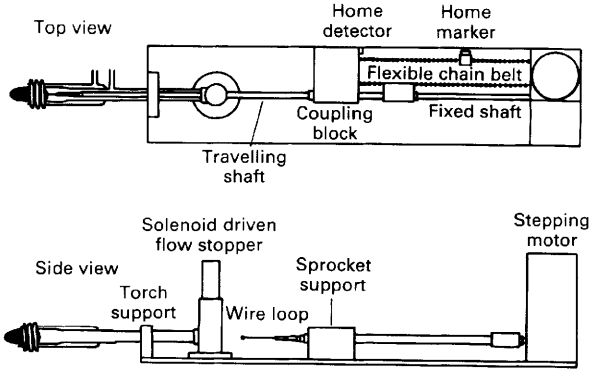

Fig. 2. Schematic diagram of the wire loop direct sample insertion device

The thermal programme used depends on the analyte, its matrix and the filament material. Whereas the drying and ashing stages are carried out slowly (about 60 s each) to prevent spitting and uneven combustion, a rapid rise in temperature is preferred in the vaporisation step where the final temperature is held, typically, for 5 s. Repetitive scans, in the multi-channel mode of data acquisition, are made at the desired masses until the accumulated dwell times of 5 or 10 ms attain the measurement time of 50 or 100 ms and this is repeated continuously throughout the duration of the peak. If measurement is made by comparison with standard solutions (external calibration) then the signal of count rate *versus* time at the selected isotope is integrated off-line using a microcomputer. If isotope dilution is the method of calibration then the analyst has the choice of taking the average of a selected number of ratios round the peak or taking the average ratio of the entire peak profile.

Wire loop DSI device

Initially, the alignment of the wire loop must be adjusted so that it is coaxial with the sampling orifice. The distance between the sampling orifice and the tip of the wire plays an important role in the signal strength. However, analyte response graphs do not differ greatly and a well defined distance of approximately 2 mm has been found to be optimum for many elements (Ag, As, Au, Cd, Cu, Li, Mn, Pb and Pd). Plasma power settings in the range 0.8–1.0 kW have provided the best signal to background ratios for most elements determined so far.

The optimum drying position depends on the auxiliary gas flow-rate as variation in the latter changes the profile of the plasma and, hence, temperature. The two parameters are chosen so that the drying stage is complete within about 40 s for a 10-μl sample, this being denoted by a decrease in the reflected power. The loop is located approximately 10–12 mm behind the base of the plasma during this step. Ashing is accomplished by inserting the wire loop further into the plasma prior to analyte vaporisation, the exact distance and duration being dependent on the sample matrix.

In this work it was found that the ion lens voltages do require re-optimisation when changing from nebulisation to DSI introduction. Response graphs for individual lenses [Einzel (EI), photon stop (S2), Bessel-box barrel (B) and Bessel-box plate (P)] and different elements are currently under investigation.

After insertion to the analyte vaporisation stage, a short delay of about 0.2 s is generally incorporated into the programme before the commencement of data acquisition. The "observation window" required for quantification is established by profiling the response of a standard solution and by a total count rate over that period used in calculation of the concentration. For most elements, the loop resides at the insertion position for only 1 s.

Advantages of DSI and ETV Over Conventional Nebulisation

Volume of solution required

Routinely, a 10-μl aliquot of solution is used for analysis with introduction by DSI or ETV. If greater sensitivity is required then replicate aliquots may be added upon drying; this is

easier to perform with the ETV device as the filament may be heated continuously during sample addition, whereas the loop in DSI introduction would need to be positioned below the plasma for drying and then brought back for further sampling. However, as both techniques provide a greater detection capability than conventional nebulisation, replicate additions are generally unnecessary. The requirement for μl rather than ml volumes of sample solution makes both techniques particularly attractive for fluid inclusion studies in geochemical applications and in the analysis of human fluids. Further, an analytical procedure may be designed so that the final volume of solution is less than 1 ml, hence minimising the dilution factor and, therefore, the detection level in the original sample.

Ease of analysis of organic solutions

The argon plasma is not an efficient medium for the oxidation of organic molecules and the cool sampling cone forms an ideal surface for carbon deposition. Both Hutton[21] and Hausler[22] have shown that addition of a small amount of oxygen to the nebuliser gas eliminates the condensation of particulate carbon (from the burnt solvent) on the sampler and skimmer and hence facilitates nebulisation of organic solvents without blockage of the orifice. The background spectra obtained when analysing, for example, a white spirit or xylene, rather than an aqueous solution, contain additional peaks due to various ArC^+ species (*m/z* 50, 51, 52 and 53) and two predominant signals at *m/z* 44 ($^{12}CO_2^+$) and *m/z* 45 ($^{12}CO_2H^+$, $^{13}CO_2^+$).

However, modification of the plasma gases or the power is not required when analysing organic solutions using DSI or ETV. In the former technique the sample is desolvated before entering the plasma, with the result that a low proportion of carbon species actually reaches the sampling orifice; in the course of this work there was no evidence of carbon condensation on the sampler after analysing isobutyl methyl ketone (IBMK) extracts for Au. In the latter technique vapours generated during the drying step are vented to waste immediately upon exit from the ETV cell. With neither technique are there additional peaks in the background spectra due to carbon species. In addition to having application to the petroleum industry, these features make DSI or ETV sample introduction attractive because analytes can be easily separated from a potentially problematic matrix into an organic solvent (such as a ketone, ester or alcohol).

Reduced oxide and hydroxide formation

In analysis by NEB-ICP-MS, significant isobaric interferences arise from oxides or hydroxides that originate either from plasma species (*e.g.*, ArO^+) or from matrix elements (*e.g.*, CaO^+ and $CaOH^+$). Beauchemin *et al.*[23] have shown that the interferences created by the presence of CaO^+ and $CaOH^+$ molecular ions on the isotopes of Ni and Co (*m/z* 58, 59, 60, 61 and 62) precluded their direct determination in the river reference material SLRS-1. The problem was solved by pre-concentration and separation of the analytes on silica-immobilised 8-hydroxyquinoline. Iron was not determined because of the overlap of ArO^+, generating a signal of 10 000–30 000 counts s^{-1}, with the major isotope (91.7% abundance) of Fe at *m/z* 56.

Because the sample has been desolvated before analysis in ETV- or DSI-ICP-MS, the population of oxide and hydroxide species is low and, therefore, isobaric interferences arising from oxides and hydroxides of matrix elements are rare. Hence the direct determination of Ni, for example in SLRS-1, is possible (see later discussion). In addition to the obvious benefit of a greatly reduced analysis time, the likelihood of contamination (a major concern when working at low analyte concentrations in waters) is minimal. The signal due to ArO^+ at *m/z* 56 remains but the count-rate is 20–30 times lower than that obtained by NEB-ICP-MS depending on the operating conditions; hence direct determination of Fe to a detection limit of about 1 ng ml^{-1} is possible.

High salt solutions

An upper limit of 0.1–0.2% total dissolved salt content is desirable in NEB-ICP-MS, not only to avoid a gradual decrease in sensitivity and eventual blockage of the sampling orifice, but also to minimise matrix-induced interferences. This is, at present, a major constraint in analysis by NEB-ICP-MS as the need to dilute sample solutions often negates the advantage of the inherent sensitivity of the technique.

The benefit of the ashing step in ETV-ICP-MS has been described in an earlier paper[13] that reported that Mo was determined accurately in solutions that contained 7% dissolved salts resulting from a carbonate fusion, thereby obviating the lengthy separation step of adsorption on to activated charcoal. Molybdenum is a relatively involatile element and hence the major constituents of the matrix (Na^+ and K^+) could be ashed completely, prior to vaporisation of the analyte. Conversely, it may be possible to vaporise a volatile analyte, leaving the bulk of the matrix to be ashed in a cleaning step following analysis. In DSI-ICP-MS ashing is performed by insertion of the loop into the plasma to a specific distance, depending on the temperature required; therefore, some of the vapours produced will be sampled by the mass spectrometer and could result in salt build-up on the orifice. This would also occur in the cleaning of the wire loop after the vaporisation of a volatile analyte. Obviously, the complete removal of vapours generated during the ashing and cleaning steps makes sample introduction by ETV preferable to DSI in the analysis of solutions of high concentrations of dissolved salts.

Matrix modification

Potential isobaric or matrix-induced non-spectral interferences can often be eliminated in ETV- or DSI-ICP-MS by matrix modification, a practice frequently employed in graphite furnace atomic absorption spectrometry (GFAAS). Ni and Shan[24] have demonstrated the use of matrix modification to achieve temporal resolution between the analyte and its matrix.

Sample introduction by ETV is preferred to that by DSI when using matrix modification, not only because of the facility to remove completely unwanted vapours formed during the ashing and cleaning steps, but also because of the enhanced ability to "fine-tune" the thermal programme applied to the sample in a well defined and reproducible manner. Further, in ETV-ICP-MS other gases may be introduced into the argon atmosphere surrounding the filament during the ashing and vaporisation steps, to aid vaporisation of either the analyte or the matrix. The introduction of hydrogen gas in GFAAS has reduced effectively the atomisation temperature of Pb.[24] Park and Hall[13] have demonstrated the benefit of introducing Freon during the vaporisation of Mo and W in ETV-ICP-MS in order to minimise carbide formation on the graphite surface. The different thermal characteristics of Ag and Pd have proved advantageous in the determination of Pd in acidic solutions derived from the dissolution of Ag prills that are formed by the classical lead fire-assay procedure in the decomposition of geological material.[25] In analysis by NEB-ICP-MS, the large excess of Ag over Pd creates a positive error on $^{106}Pd^+$ due to the tailing effect of $^{107}Ag^+$ on the low mass side. However, analysis by ETV-ICP-MS is interference-free because Ag is vaporised completely before Pd. This would also occur with DSI-ICP-MS as an ashing step could be incorporated prior to vaporisation.

Clearly, the large amount of information amassed during studies of GFAAS and ETV-ICP-AES will be useful in both ETV- and DSI-ICP-MS.

Results and Discussion

Analysis of the River Water Reference Material SLRS-1

To compare the advantages and limitations of the ETV and DSI introduction techniques, the river water reference sample SLRS-1 (NRCC, Ottawa, Canada) was analysed 10 times for the elements Mn, Pd, Au, As, Fe, Ni and Mo using simple external calibration at the most abundant isotope. The standard solutions used for calibration were acidified to 1% HNO_3, so as to correspond to SLRS-1, for all elements except Au, for which extraction into IBMK was performed from a solution 2 M in HCl. The most suitable substrate (graphite, tantalum, tungsten or rhenium) was chosen for the filament material used in the ETV studies, whereas only tungsten was available as the loop material in the DSI work. This proved to be a limiting factor for DSI as impurities of Fe, Ni and Mo were found in the tungsten loop (Fig. 3). Unfortunately, the signals obtained for Fe, Ni and Mo by replicate insertions of the loop alone were not consistent and estimation of a background value was impossible. An alternative supply of the tungsten material was located but it also contained these impurities. Other materials which will maintain their shape in the horizontal plane are currently being investigated in the DSI work. The detection limit used to compare the techniques may be defined as that concentration of analyte equivalent to three times the standard deviation of the blank (1% HNO_3), which was measured 10 times in succession. This basis for comparison favours NEB-ICP-MS because the time required to analyse a solution 10 times is far shorter than that needed by DSI- or ETV-ICP-MS (50 s as against 15–20 min), hence longer term drift does not degrade the result.

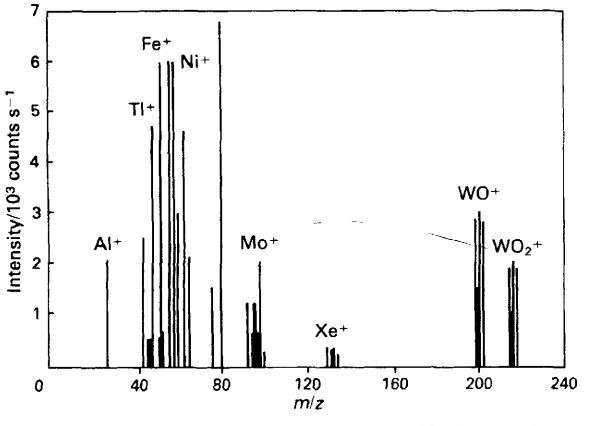

Fig. 3. Scan of the "blank" tungsten loop in DSI-ICP-MS, showing impurities of Fe, Ni and Mo

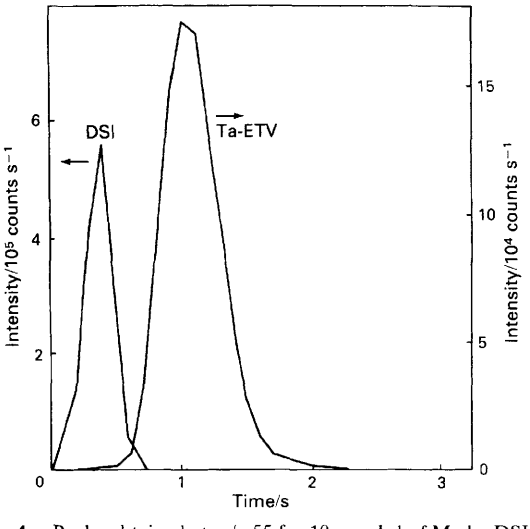

Fig. 4. Peaks obtained at *m/z* 55 for 10 ng ml^{-1} of Mn by DSI- and ETV-ICP-MS. Sample aliquots: 10 µl for DSI; 5 µl for ETV from a tantalum filament

Manganese

The peak profiles for a 10 ng ml^{-1} Mn standard solution obtained by DSI- and ETV-ICP-MS are similar in shape, whereas the duration differs by a factor of two (Fig. 4). For ETV, tantalum was found to be preferable to graphite as tailing occurred with the latter prolonging the peak width to about 2.5 s. The peak generated by the electrothermal vaporisation of SLRS-1 was broader than those of the standard solutions in 1% HNO_3 (Fig. 5). An even broader peak was obtained for the sea water reference sample CASS-1. In order to minimise errors caused by the matrix composition of the sample, calibration was carried out by the method of standard additions. Three solutions were analysed, SLRS-1, SLRS-1 + 2 ng ml^{-1} Mn and SLRS-1 + 4 ng ml^{-1} Mn. Each solution was analysed in triplicate and the entire procedure repeated five times. The precision, expressed as RSD, for each solution was in the range 1–4%. The results, together with those obtained by DSI- and NEB-ICP-MS for which external calibration was used, are shown in Table 1. Good agreement with the certified value of 1.77 ± 0.23 ng ml^{-1} was obtained by NEB- and ETV-ICP-MS but a slightly low value of 1.43 ± 0.17 ng ml^{-1} was obtained by DSI-ICP-MS. A downward drift in signal was experienced for SLRS-1 in the DSI work, which probably explains this result. A possible cause could be a broadening of the peak relative to the integration period as established by the calibration solutions and, hence, low quantification of the real peak, as occurs in ETV-ICP-MS (Fig. 5). The precision of 10 replicate analyses of the 10 ng ml^{-1} standard solution by DSI-, ETV- and NEB-ICP-MS was 5, 3 and 1%, respectively.

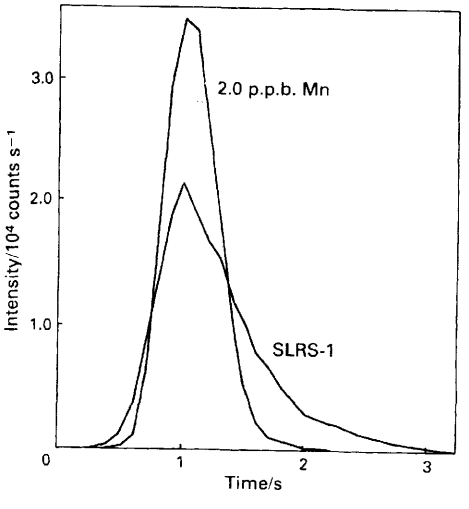

Fig. 5. Peaks obtained at *m/z* 55 for 2 ng ml^{-1} of Mn and river water reference material, SLRS-1, by ETV-ICP-MS

Table 1. Analysis of SLRS-1 for Mn by ICP-MS; n = 5, external calibration for NEB and DSI, standard addition for ETV. Certified value for SLRS-1 = 1.77 ± 0.23 ng ml^{-1}

	Mn/ng ml^{-1}		
	DSI	ETV	NEB
SLRS-1	1.43 ± 0.17	1.83 ± 0.10	1.73 ± 0.10
DL	0.05	0.02	0.20

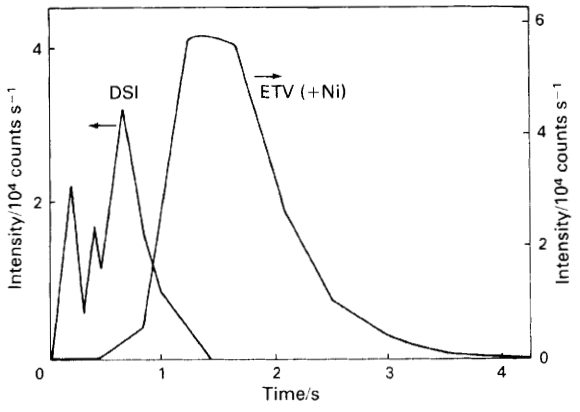

Fig. 6. Peaks obtained at *m/z* 105 for 10 ng ml^{-1} of Pd by DSI- and ETV-ICP-MS. Sample aliquots: 10 µl for DSI; 3 µl for ETV from a graphite platform + 3 µl of 500 µg ml^{-1} of Ni as matrix modifier

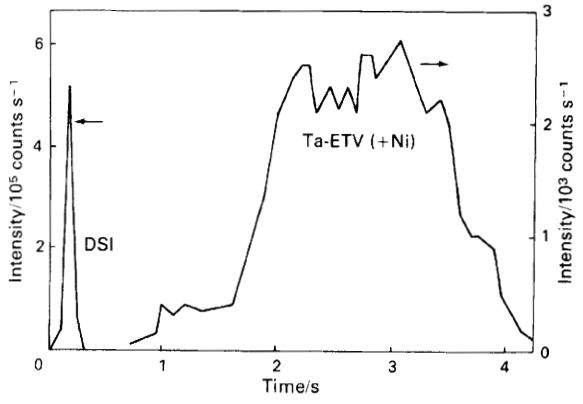

Fig. 7. Peaks obtained at *m/z* 75 for 10 ng ml^{-1} of As by DSI- and ETV-ICP-MS. Sample aliquots: 10 µl for DSI; 3 µl for ETV from a tantalum filament + 3 µl of 500 µg ml^{-1} of Ni as matrix modifier

Table 2. Analysis of SLRS-1 for Pd by ICP-MS; n = 10, external calibration

	Pd/ng ml^{-1}		
	DSI	ETV	NEB
SLRS-1	0.043 ± 0.013	<0.06	0.26 ± 0.01
DL	0.004	0.06	0.15

Table 3. Analysis of SLRS-1 for As by ICP-MS; n = 5, external calibration. Certified value for SLRS-1 = 0.55 ± 0.08 ng ml^{-1}

	As/ng ml^{-1}		
	DSI	ETV	NEB
SLRS-1	0.49 ± 0.03	0.63 ± 0.07	0.58 ± 0.08
DL	0.2	0.3	0.3

Palladium

Fig. 6 shows the signals obtained at *m/z* 105 by DSI- and ETV-ICP-MS for a 10 ng ml^{-1} Pd standard solution in 1% HNO_3. Whereas a sample aliquot of 10 µl was taken for introduction by DSI, a volume of only 3 µl was used for ETV to which was added a second 3-µl aliquot of a 500 µg ml^{-1} Ni (as nitrate) solution. The presence of Ni not only improved the reproducibility of vaporisation of Pd from the graphite substrate but also enhanced the signal by a factor of four. It is thought that the binding of Pd with Ni minimises reduction of Pd on graphite and the formation of the carbide species; hence, a smooth, single peak of about 3 s duration is obtained. At least two peaks are discernible in the spectrum obtained from vaporisation by DSI, probably owing to the formation of different Pd intermediate species, and the duration of the signal (almost 1.5 s) is much longer than that of the other elements determined. It is interesting to note the matrix effect of 500 µg ml^{-1} of Ni on Pd by DSI-ICP-MS: a three-fold suppression was observed. By adjusting plasma conditions and the insertion position the signal could be improved, but to a maximum of only 60% of that in the absence of 500 µg ml^{-1} of Ni. Similarly, under conditions which are optimum for the sensitivity of Pd, the presence of 500 µg ml^{-1} of Ni in NEB-ICP-MS suppresses the count rate observed for 10 ng ml^{-1} of Pd to 63% of that without Ni. This similarity of suppression by Ni in DSI- and in NEB-ICP-MS suggests that a much lower relative amount of Ni is being sampled concurrently with Pd in ETV-ICP-MS, that is, the two elements are thermally differentiated during the heating programme. Further experiments indicated that most of the Ni was vaporised during the ashing stage in ETV-ICP-MS.

The precision obtained for 10 replicate determinations of a 10 ng ml^{-1} Pd solution by DSI- and ETV-ICP-MS was 4 and 6%, respectively, at *m/z* 105. The detection limits are considerably better than that of nebulisation (Table 2).

The results of the analysis of SLRS-1 are shown in Table 2. The high and erroneous value of 0.26 ± 0.01 ng ml^{-1} of Pd obtained by NEB is due to the isobaric interference of $^{88}Sr^{16}O^{1}H^{+}$ on $^{105}Pd^{+}$; SLRS-1 contains 136 ng ml^{-1} of Sr. No such effect was encountered in the determination of Pd by DSI- or ETV-ICP-MS in the presence of 1, 10 or 100 µg ml^{-1} of Sr. Similarly, Y (*m/z* 89, 100% abundance) causes an isobaric interference on $^{105}Pd^{+}$ as the oxide $^{89}Y^{16}O^{+}$. Under optimum conditions for Pd, 10 ng ml^{-1} of Y gives an apparent signal for Pd of about 1 ng ml^{-1} by NEB-ICP-MS. Again, there is no interference by DSI- or ETV-ICP-MS, due to the much reduced population of O and OH radicals. Whereas the response for Pd in SLRS-1 was below the detection limit of 0.06 ng ml^{-1} for ETV-ICP-MS, the concentration determined by DSI-ICP-MS was 0.043 ± 0.013 ng ml^{-1}. Although SLRS-1 is not certified for Pd, we doubt the presence of detectable Pd in St. Lawrence river water because the concentration of this element in waters collected in areas of near-surface Pd deposits (*e.g.*, Rottenstone Deposit, Saskatchewan, Canada) is below 0.02 ng ml^{-1}.[26] It is thought that the high result obtained by DSI-ICP-MS could be due to a memory effect on the tungsten loop because SLRS-1 was analysed after a Pd standard of 100 ng ml^{-1}; this is currently under investigation.

Arsenic

The peak shapes obtained by the two techniques differ greatly for the volatile element As (Fig. 7). Vaporisation by DSI results in a sharp peak of only 0.25 s duration, whereas ETV from a tantalum filament results in a broad, slightly erratic peak lasting over 3 s. The sample aliquot taken for ETV was reduced to 3 µl in order to accommodate an additional 3 µl of 500 µg ml^{-1} Ni (as the nitrate) solution. In the absence of Ni, severe memory effects were encountered due to the analyte adsorbing on the walls of the tubing in its passage to the ICP. This was evidenced by the peaks obtained when firing the blank furnace, with a minimum application of heat during the vaporisation cycle (*ca.* 100 °C), following analysis of a 10 ng ml^{-1} As standard solution. Matrix modification with Ni appeared to solve this transport problem and the memory effect was not observed. However, even with maximisation of the ramp rate from the ash to the vaporisation cycle, a broad, undesirable signal was obtained. Similar behaviour was observed when a graphite filament was used. Frequent re-calibration was found to be necessary for both introduction

systems used in the determination of As; typically, a 10% change in sensitivity could be experienced after 5–10 analyses.

Five replicate analyses of the 10 ng ml^{-1} As standard solution gave an RSD of 6% for both DSI and ETV; this compares with about 1% over the short term by NEB-ICP-MS. Although the sensitivity achieved by DSI is superior to that of NEB-ICP-MS (*e.g.*, a peak height for 10 ng ml^{-1} of 5×10^5 counts s^{-1} compared with a steady-state intensity of about 1×10^3 counts s^{-1}), the greater noise factor encountered in DSI at low concentrations of As (0.1–0.2 ng ml^{-1}) tends to offset this advantage. Hence, the detection limits are similar (0.2–0.3 ng ml^{-1} of As) for all three techniques (Table 3). The results of the analyses of SLRS-1, given in Table 3, agree favourably with the certified value of 0.55 ± 0.08 ng ml^{-1}. Because SLRS-1 was acidified with nitric rather than hydrochloric acid no interference was observed from $^{40}Ar^{35}Cl^+$ at *m/z* 75, as confirmed by Beauchemin *et al.*[23] in the analysis of SLRS-1 by standard-additions NEB-ICP-MS after a 20-fold concentration procedure via evaporation. The RSD obtained by Beauchemin *et al.* was 4% for SLRS-1, only slightly better than that obtained by the best direct technique for As in this work, *i.e.*, 6% by DSI-ICP-MS.

Gold

Owing to the low natural abundance of gold (2.5 ng g^{-1})[27] the detection limit required for geochemical exploration studies is about 1 ng g^{-1} for solid samples (rocks, soils and sediments) and 1 ng l^{-1} for waters. Hence, analytical techniques in common use require a concentration and separation procedure. This is often accomplished, following solubilisation of Au, by a simple extraction of the complex $AuCl_4^-$ into IBMK.[26,28] The following indicates the ease with which organic solutions can be analysed by DSI- and ETV-ICP-MS without the deleterious effect of condensation of carbon particles on the sampler, skimmer and lens surfaces. Analysis of organic solvents by NEB-ICP-MS would require the addition of oxygen to the nebuliser gas and a higher than usual plasma power of 1.5–1.8 kW.

The signals obtained from a 10 ng ml^{-1} Au standard solution in IBMK by DSI- and ETV-ICP-MS (with a rhenium filament) are shown in Fig. 8. Both peaks are smooth and the ETV signal lasts about seven times longer than the DSI signal of only 0.3 s. Excellent sensitivity is achieved by both techniques, as is apparent from the peak heights of 3×10^5 and 7×10^4 counts s^{-1} for the 10 ng ml^{-1} standard by DSI- and ETV-ICP-MS, respectively. A steady-state signal of about 6×10^3 counts s^{-1} is obtained by nebulisation of a 10 ng ml^{-1} aqueous solution and an RSD of about 5%. Ten replicate analyses of the 10 ng ml^{-1} organic standard resulted in RSDs of 2 and 3% by DSI- and ETV-ICP-MS, respectively.

The detection limit for Au in IBMK by DSI is excellent, being 0.002 ng ml^{-1}, and that by ETV-ICP-MS is 0.008 ng ml^{-1}. These are at least a factor of ten better than that (0.07 ng ml^{-1}) obtained by NEB-ICP-MS using aqueous solutions. Replicate analyses (10) of the IBMK extract of SLRS-1 (acidified to 2 M HCl) gave results from below the detection limit to 0.01 ng ml^{-1} by both techniques; this positive value was probably due to the error in measuring the small blank contamination arising from HCl.

Iron, molybdenum and nickel

Although the presence of impurities in the tungsten loop precluded the determination of Fe, Mo and Ni in this work, sample introduction by DSI should show similar advantages to ETV, namely, reduced oxide and hydroxide populations at, for example, *m/z* 56 (ArO^+), 60 (CaO^+) and 61 ($CaOH^+$). Iron has been determined directly by ETV-ICP-MS in SLRS-1 at the GSC laboratory to give 32.1 ± 3.1 ng ml^{-1} ($n = 5$) by external calibration at *m/z* 56 (certified value 31.5 ± 2.1 ng ml^{-1}). The RSD is much improved (to ±2–3%) if isotope dilution ($^{56}Fe^+ : {}^{57}Fe^+$ measured) is used. Similarly, Ni has been determined directly in SLRS-1 by isotope-dilution ETV-ICP-MS, using the ratio $^{60}Ni^+ : {}^{61}Ni^+$, without the need for CaO^+ or $CaOH^+$ correction. The result of 1.15 ± 0.05 ng ml^{-1} ($n = 5$) compares favourably with the certified value of 1.07 ± 0.06 ng ml^{-1}.

The peak obtained by the vaporisation of a 10 ng ml^{-1} standard solution of Mo using sample introduction by DSI is shown in Fig. 9, together with the corresponding signal produced by ETV. The initial sharp peak due to the sample is noted followed by what appears to be a steady-state signal due to the Mo in the tungsten loop. As expected, the peak width of Mo vaporised from a graphite platform in ETV introduction is much broader, even in an atmosphere containing Freon. It remains to be seen whether Mo is completely vaporised from tungsten in the plasma or whether a memory effect is present in analysis by DSI-ICP-MS.

Conclusions

The wire loop DSI device is simpler in design and less expensive to construct than its ETV counterpart. The duration of the peak is much shorter, generally by a factor of 2–10, hence peak heights obtained by DSI can be expected to be significantly greater than those obtained by ETV. The entire sample is presented for vaporisation whereas the transport efficiency by ETV introduction is generally of the order of 60–80%. Severe memory effects can be encountered with some elements, such as As, in passage from the ETV cell to

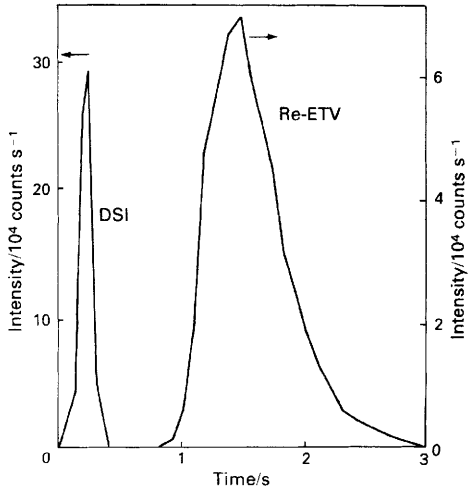

Fig. 8. Peaks obtained at *m/z* 197 for 10 ng ml^{-1} of Au (in IBMK) by DSI- and ETV-ICP-MS. Sample aliquots: 10 µl for DSI; 10 µl for ETV from a rhenium filament

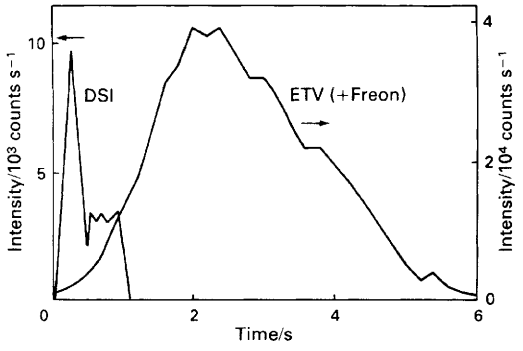

Fig. 9. Peaks obtained at *m/z* 95 for 10 ng ml^{-1} of Mo by DSI- and ETV-ICP-MS. Sample aliquots: 10 µl for DSI; 10 µl for ETV from a graphite platform with halide-assisted vaporisation by addition of 0.2% Freon

the plasma and the severity may depend on the sample matrix. Changes in transport efficiency will obviously reduce the precision of results obtained in ETV studies and, for this reason, isotope dilution is the preferred method of calibration. An absence of transport problems is a major advantage of DSI introduction.

Although better precision and detection limits may be anticipated using DSI in the analysis of relatively "clean" and dilute solutions (*e.g.*, most non-saline surface waters), the ETV technique has greater flexibility in providing accurate analysis of more complex solutions that contain high concentrations of total dissolved salts. Not only can salt build-up on the sampling orifice be eliminated, but potential interferences can be removed by careful control of the thermal programme and modification of the matrix. Hence, at this stage of development, the ETV technique is superior for application to solutions such as acid leachates of geological materials. Similarly, it would probably have a small advantage in the routine analysis of organic solutions due to its being able to vent to waste organic-laden vapours. The use of tungsten as the loop material has several limiting factors: it precludes the determination of highly involatile elements, those elements isobaric with WO^+ and WO_2^+ and those elements which exist as impurities within the wire itself (*e.g.*, Fe, Ni and Mo).

Both ETV and DSI techniques have the advantages over conventional pneumatic nebulisation in analysis by ICP-MS of a low sample-volume requirement, greatly reduced oxide and hydroxide formation and improved detection limits.

Future Directions

It is apparent from this work that, in order to expand the application of the DSI technique, different materials must be investigated. A difficulty which may arise with other metals, such as tantalum and rhenium, is their inability to maintain rigidity under frequent motion in the horizontal rather than the vertical plane after repeated exposure to intense heat. Graphite cups similar to those designed for ICP-AES studies[29] should be investigated; a widening of the peak shape, similar to that shown in profiles of ETV introduction, will probably occur owing to the higher thermal mass of the graphite itself. The possibility of direct solid-sample analysis will be feasible with the advent of graphite cups, although blockage of the sampling orifice will be a limiting factor as will the representativeness of mg sample masses. Work is in progress at the GSC on the direct analysis of sea water evaporates by ETV-ICP-MS[30] using isotope dilution as the method of calibration.

The graphite platforms used in ETV studies at present are not ideal: their lifetime is short and the spreading of highly acidic solutions from the centre towards the electrodes results in uneven vaporisation. Totally pyrolytic platforms do not heat uniformly and various thicknesses of coating (25 μm and greater) are being tested. Some success has been achieved in attempting to restrict the sample volume to the central region by V- and U-shaped graphite but further investigation is being carried out. Refinements in these areas should improve the reproducibility of analysing acidic solutions which are not compatible with vaporisation from metal filaments.

The main disadvantage of both techniques, compared with nebulisation, is speed. This is being addressed, at least partly, by automation which is taking place at our two laboratories. Current limitations in the software offered by Perkin-Elmer/SCIEX preclude the determination of more than four isotopes per analysis, although for extremely rapid signals, such as those produced in the DSI technique, the limitation probably lies in the scanning rate of the spectrometer.

References

1. Vaughan, M. A., and Horlick, G., *Appl. Spectrosc.*, 1986, **40**, 434.
2. Tan, S. H., and Horlick, G., *Appl. Spectrosc.*, 1986, **40**, 445.
3. Tan, S. H., and Horlick, G., *Appl. Spectrosc.*, 1988, in the press.
4. Beauchemin, D., McLaren, J. W., and Berman, S. S., *Spectrochim. Acta, Part B*, 1987, **42**, 467.
5. Gregoire, D. C., *Spectrochim. Acta, Part B*, 1987, **42**, 895.
6. Tan, S. H., and Horlick, G., *J. Anal. At. Spectrom.*, 1987, **2**, 745.
7. Vaughan, M.-A., Horlick, G., and Tan, S. H., *J. Anal. At. Spectrom.*, 1987, **2**, 765.
8. Gray, A. L., and Williams, J. G., *J. Anal. At. Spectrom.*, 1987, **2**, 599.
9. Zhu, G., and Browner, R. F., *Appl. Spectrosc.*, 1987, **41**, 349.
10. Jiang, S.-J., and Houk, R. S., *Spectrochim. Acta, Part B*, 1987, **42**, 93.
11. Williams, J. G., Gray, A. L., Norman, P., and Ebdon, L., *J. Anal. At. Spectrom.*, 1987, **2**, 469.
12. Arrowsmith, P., *Anal. Chem.*, 1987, **59**, 1437.
13. Park, C. J., and Hall, G. E. M., *J. Anal. At. Spectrom.*, 1987, **2**, 473.
14. Park, C. J., and Hall, G. E. M., *J. Anal. At. Spectrom.*, 1988, **3**, 355.
15. Park, C. J., Van Loon, J. C., Arrowsmith, P., and French, J. B., *Anal. Chem.*, 1987, **59**, 2191.
16. Date, A. R., and Cheung, Y. Y., *Analyst*, 1987, **112**, 1531.
17. Boomer, D. W., Powell, M., Sing, R. L. A., and Salin, E. D., *Anal. Chem.*, 1986, **58**, 975.
18. Matusiewicz, H., *J. Anal. At. Spectrom.*, 1986, **1**, 171.
19. Salin, E. D., and Sing, R. L. A., *Anal. Chem.*, 1984, **56**, 2596.
20. Park, C. J., and Hall, G. E. M., *Geol. Surv. Can. Pap.*, 1986, 86–1B, 767.
21. Hutton, R. C., *J. Anal. At. Spectrom.*, 1986, **1**, 259.
22. Hausler, D., *Spectrochim. Acta, Part B*, 1987, **42**, 63.
23. Beachemin, D., McLaren, J. W., Mykytiuk, A. P., and Berman, S. S., *Anal. Chem.*, 1987, **59**, 778.
24. Ni, Z.-M., and Shan, X.-Q., *Spectrochim. Acta, Part B*, 1987, **42**, 937.
25. Hall, G. E. M., Pelchat, J. C., and Park, C. J., paper presented at the 1988 Winter Conference on Plasma Spectrochemistry, San Diego, CA, USA, 3rd–9th January, 1988, paper Th 15.
26. Hall, G. E. M., and Bonham-Carter, G. F., *J. Geochem. Explor.*, 1988, in the press.
27. Elson, C. M., and Chatt, A., *Anal. Chim. Acta*, 1983, **155**, 305.
28. Hall, G. E. M., Vaive, J. E., and Ballantyne, S. B., *J. Geochem. Explor.*, 1986, **26**, 191.
29. Monasterios, C. V., Jones, A. M., and Salin, E. D., *Anal. Chem.*, 1986, **58**, 780.
30. Park, C. J., and Hall, G. E. M., paper presented at the XXV Colloquium Spectroscopicum Internationale, Toronto, Canada, 21st–26 June, 1987, paper E4.3.

Paper 8/00630J
Received February 18th, 1988
Accepted April 26th, 1988